

Magnetic coupling between Cr atoms doped at bulk and surface sites of ZnO

Q. Wang, Q. Sun, and P. Jena^{a)}

Physics Department, Virginia Commonwealth University, Richmond, Virginia 23284

Y. Kawazoe

Institute for Material Research, Tohoku University, Sendai 980-8577, Japan

(Received 24 January 2005; accepted 9 September 2005; published online 12 October 2005)

Contrary to theoretical prediction that Cr-doped bulk ZnO is ferromagnetic, recent experiments on Cr-doped ZnO thin film reveal the coupling to be antiferromagnetic. Using first-principles calculations based on gradient corrected density functional theory, we show that a possible origin of this disagreement may be associated with the site preference of Cr. In bulk, when Cr substitutes Zn, bond contraction occurs and Cr atoms prefer to cluster around O atoms. The ferromagnetic coupling among Cr atoms is driven by Cr 3*d* and O 2*p* exchange interactions as in Cr₂O cluster. However, when Cr atoms replace Zn on the surface, due to the different bonding environment, bonds expand preventing Cr atoms from clustering around O atoms. Consequently, the coupling between Cr atoms becomes antiferromagnetic. © 2005 American Institute of Physics. [DOI: 10.1063/1.2106023]

Dilute magnetic semiconductors (DMS) have been regarded as prime candidates for applications in spintronics. Among the extensively studied DMS systems, GaMnAs,¹ InMnAs,² and ZnCrTe³ have been found to exhibit ferromagnetic order unambiguously. Following the theoretical predictions^{4–6} of ferromagnetism in Cr-doped bulk ZnO, considerable experimental efforts have been devoted to this system.^{7–11} Using a pulsed-laser deposition technique, Ueda and co-workers⁷ prepared ZnO film doped with 3*d* transition metals including Co, Mn, Cr, and Ni. They found that Cr, Ni and Mn-doped ZnO films did not show ferromagnetic behavior. Jin *et al.* also did not find any indication of ferromagnetism for Cr-doped ZnO film at low temperature even down to 3 K.⁸ Lee and co-workers recently reported that Cr-doped ZnO film shows no ferromagnetic behavior, and co-doping is necessary to make this system ferromagnetic.⁹ To understand these experimental results, we have performed extensive theoretical studies of Cr-doped ZnO both in the crystal and thin film.

The calculations were carried out using density functional theory (DFT) and generalized gradient approximation (GGA) for exchange and correlation. We have studied the magnetic properties of Cr-doped ZnO in both bulk and (10 $\bar{1}0$) surface with wurtzite structure. For bulk calculation, we have used (2 × 2 × 2) supercell with experimental lattice constants ($a=b=3.249$ Å, $c=5.205$ Å). We have simulated the ZnO (10 $\bar{1}0$) surface by a slab model consisting of eight layers. The corresponding ZnO supercell consists of 32 Zn atoms and 32 O atoms. Each slab was separated from the other by a vacuum region of 10 Å so that the surfaces do not interact with each other. To preserve symmetry, the top and bottom layers of the slab were taken to be similar. The central four layers of the slab were held fixed at their bulk configuration while the surface and subsurface layers on either side of the slab were allowed to relax without any symmetry constraint. The calculations of total energies and forces, and

optimizations of geometry, were carried out using DFT and PW91 functional¹² for the GGA to exchange and correlation potential. A plane-wave basis set and the projector augmented wave potentials¹³ for Cr, Zn, and O, as implemented in the Vienna *ab initio* simulation package,¹⁴ were employed. The energy cutoff was set at 300 eV and the convergence in energy and force were 10⁻¹ and 10⁻³ eV/Å, respectively. *k*-point convergence was achieved with 5 × 5 × 4 Monkhorst–Pack mesh¹⁵ for the bulk calculations. For the surface case, we used 6 × 4 × 1 Monkhorst *k* points mesh for the geometry optimization and 8 × 6 × 2 for the final calculation.

We begin our discussion with Cr-doped ZnO bulk. Figure 1(a) shows ZnO (2 × 2 × 2) supercell in wurtzite structure containing 16 Zn and 16 O atoms. To study the magnetic coupling between Cr atoms, we replaced two Zn atoms with Cr in different Zn sites which formed Zn₁₄Cr₂O₁₆ supercell. This corresponds to a 12.5% Cr concentration. Due to the wurtzite structure, [0001] direction is different from [10 $\bar{1}0$] and [01 $\bar{1}0$] directions. We, therefore, studied the relative sta-

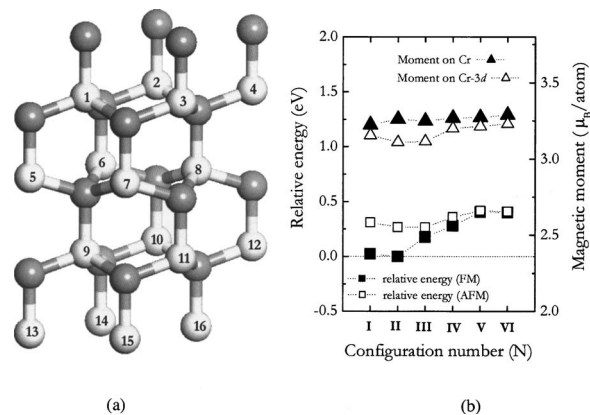


FIG. 1. (a) The (2 × 2 × 2) supercell of bulk ZnO consisting of 16 Zn and 16 O atoms. The numbered lighter spheres are Zn. The darker spheres are O. (b) Magnetic moments and relative energies calculated with respect to the ground state of Zn₁₄Cr₂O₁₆ supercell corresponding to FM and AFM states for each configuration.

^{a)} Author to whom correspondence should be addressed; electronic mail: pjena@vcu.edu

bility of Cr atoms by replacing two Zn atoms in six different configurations. Configuration I–VI correspond to Cr atoms substituting Zn at sites marked Nos. (7, 6), (7, 8), (7, 11), (7, 10), (7, 15), and (7, 12) in Fig. 1(a), respectively. In the first three configurations, Cr atoms cluster around O, namely, Cr–O–Cr, while in the last three configurations, the two Cr atoms are separated with the configuration of Cr–O–Zn–O–Cr along different directions. We calculated the total energies of ferromagnetic (FM) and antiferromagnetic (AFM) spin alignment for each configuration.

The calculations were first carried out by not allowing the supercell to relax. From this unrelaxed calculation, it was found that configuration I and II are energetically nearly degenerate and are lower in energy than the other four configurations (III–VI) by 0.238, 0.486, 0.388, and 0.438 eV, respectively. This suggests that occupancy of Cr is anisotropic and Cr atoms have a tendency to cluster around O atoms in bulk ZnO. The energy difference between the AFM and FM states ($\Delta E = E_{\text{AFM}} - E_{\text{FM}}$) is 0.285, 0.285, 0.191, 0.090, 0.072, and 0.023 eV for configurations I–VI, respectively. This verifies that the coupling between these two Cr atoms is FM as predicted by previous theoretical studies.^{4–6} This FM coupling feature between Cr atoms in bulk ZnO is analogous to that in Cr₂O cluster where the O atom mediates the magnetism through *p-d* exchange interactions.¹⁶

We then allowed all the atoms in the Zn₁₄Cr₂O₁₆ supercell to fully relax without any symmetry constraint. Configuration II was found to be the ground state lying 0.021, 0.177, 0.279, 0.404, and 0.403 eV lower in energy than configurations I, III, IV, V, and VI, respectively. The FM state lies 0.288, 0.267, 0.089, 0.080, 0.064, and 0.044 eV lower in energy than the AFM one for configuration I–VI, respectively. Therefore, the optimization of the supercell in ZnO bulk did not change the FM coupling characteristics. In the ground state, the magnetic moment on Cr atom is found to be 3.26 μ_B and arises mainly from Cr 3*d* orbital (3.11 μ_B). A small contribution to the moment results from 4*s* (0.12 μ_B) and 4*p* (0.04 μ_B) orbitals of Cr due to the *sp* and *d* hybridization. The O atom bridging the two Cr atoms is antiferromagnetically polarized and carries a magnetic moment of $-0.05 \mu_B$ mainly coming from O 2*p* orbitals. The overall magnetic moment at each Cr atom is about 3.20 μ_B (as plotted in Fig. 1(b)) and the two Cr atoms couple ferromagnetically to each other but antiferromagnetically to their nearest neighbor O atoms. The hybridization between O 2*p* and Cr 3*d* reduces the magnetic moment of Cr as compared to that of a free Cr atom.

The electronic structure of Cr-doped bulk ZnO can be seen from Figs. 2(a) and 2(b). Here we only show the total density of states (DOS) and the partial DOS of Cr 3*d* and O 2*p* for the ground state configuration of fully relaxed Zn₁₄Cr₂O₁₆ supercell. The DOS shows signature of half metallic character. Most of the magnetic moment is due to contribution of Cr 3*d* states and ferromagnetism is a consequence of overlap between Cr 3*d* and O 2*p* states. The Cr–Cr and Cr–O bond lengths were found to be 3.256 and 1.982 Å, which are contracted by 1.2% and 1.0%, respectively, as compared to the undoped case. The bond length contraction is due to the fact that the electronegativity of Cr is smaller than that of Zn. Thus, when Cr replaces Zn, more charges are transferred to the surrounding O atoms resulting in a reduction of the radius of Cr compared to that of Zn.

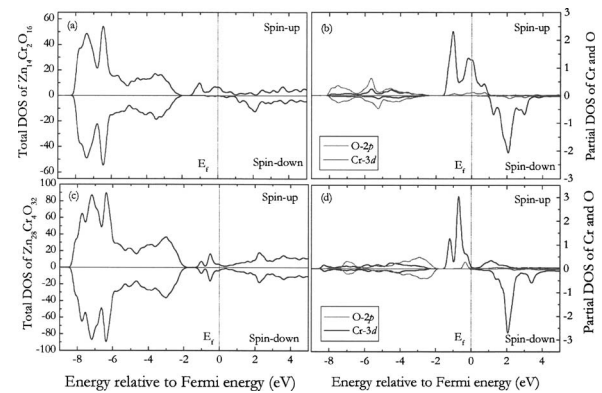


FIG. 2. (a) Total spin density of states (DOS) of the Zn₁₂Cr₂O₁₆ bulk supercell; (b) partial DOS of Cr 3*d* and O 2*p* in Zn₁₂Cr₂O₁₆ bulk; (c) total spin DOS of the Zn₂₈Cr₄O₃₂ surface supercell; (d) partial DOS of Cr 3*d* and O 2*p* in Zn₂₈Cr₄O₃₂.

We now discuss the magnetic coupling between Cr atoms on the ZnO surface. In Fig. 3 we show the supercell of the slab used to model the ZnO surface having [10 $\bar{1}$ 0] orientation. The supercell consists of 32 Zn atoms (which are lighter and marked) and 32 O atoms (which are darker). The reconstruction of the ZnO (10 $\bar{1}$ 0) surface has been discussed in our previous work.¹⁷ To study the magnetic properties of Cr-doped ZnO, we first determine the preferred site of Cr atom by substituting one Zn atom with Cr. We have considered two different configurations by replacing Zn with Cr in the surface site (marked No. 4) and subsurface site (marked No. 7) in Fig. 3. To preserve symmetry, we replaced Zn sites on the bottom two layers of the slab, namely, Nos. 31 and 25, respectively. Thus, the supercell consists of Zn₃₀Cr₂O₃₂ corresponding to a Cr concentration of 6.25%. Since the two Cr atoms in the top and bottom layers of the slab are far apart (8.968 Å), one can assume that they do not interact with each other. Thus, the above supercell geometry can give us information on the site preference of Cr in the dilute limit. The total energy of the slab with Cr substituted on the surface site was found to be 0.57 eV lower than that when Cr atom substitutes the subsurface site. This shows that Cr prefers to reside on the surface site, similar to what was found in Mn-

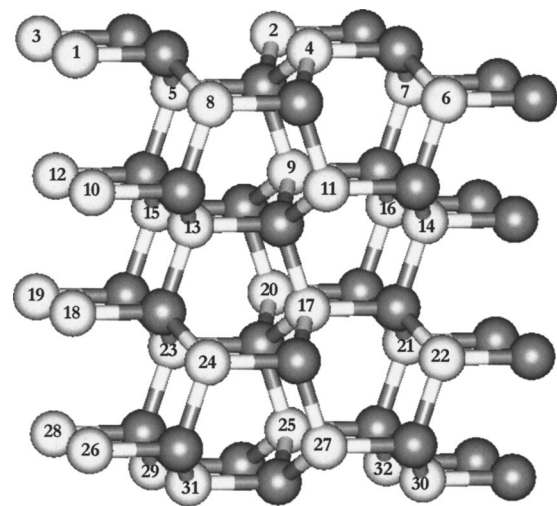


FIG. 3. The side view of the eight layer slab of (2 × 2) (10 $\bar{1}$ 0) ZnO surface consisting of 32 Zn and 32 O atoms. The numbered lighter spheres are Zn. The darker spheres are O.

doped GaN film.¹⁷ It is interesting to mention that in (Zn, Mn)O thin film, the Mn atoms did not exhibit any site preference, as the Mn occupying the surface site lies only 0.01 eV below the subsurface site.¹⁸

To determine the magnetic coupling between Cr atoms, it is necessary to replace at least two Zn atoms with two Cr on either side of the slab. This corresponds to a supercell consisting of $\text{Zn}_{28}\text{Cr}_4\text{O}_{32}$ and a Cr concentration of 12.5%. We have considered seven configurations. For each configuration, we optimized the structure fully and performed the calculations for both FM and AFM spin configurations. In the first column of Table I, we show, for each of the seven configurations, which Zn sites (see Fig. 3) have been replaced with Cr. The ground state of this system is found to be configuration III. The two Cr atoms on the surface do not form nearest neighbors suggesting that Cr atoms do not have the tendency to cluster on the surface as they did in the bulk. The optimized Cr–Cr distances are given in the second column of Table I. Using configuration III as the reference state, the energy difference $\Delta\varepsilon$ for other configurations is listed in the third column. The energy difference ΔE between the FM and the AFM states for each of the configuration is given in the fourth column of Table I. Note that the ground state is found to be AFM. Because of the surface relaxation the average Cr–O bond length on the surface is 1.939 Å. This corresponds to a 2.2% contraction, as compared to that in the ZnO bulk. The corresponding FM state is 0.025 eV higher in energy than AFM state. The configurations with two Zn atoms replaced in the subsurface layer, namely configurations VI and VII, have much higher energy than the ground state configuration III, as shown in Table I. Similarly, the energy of configurations IV and V (where one Cr atom is on the surface and the second one in the subsurface layer) is higher than the ground state configuration III by 0.857 and 0.906 eV, respectively. This once again indicates that Cr atoms prefer the surface sites of ZnO thin film. The energy difference between the FM and AFM states, that ΔE increases when the distance between Cr atoms decreases. Especially, if the two Cr atoms are substituted at the nearest neighbor sites in the same layer or different layers (configuration I, configuration VI, and configuration IV), the system displays ferromagnetism, but their energies are higher than the ground state by 0.314, 1.397, and 0.857 eV, respectively.

The total DOS and the partial spin DOS of Cr 3*d* and O 2*p* for the ground state configuration are shown in Figs. 2(c) and 2(d). Since the spin up and spin down DOS are identical as shown in Fig. 2(c), the total moment of the system is zero and the coupling between Cr atoms is AFM. The magnetic moment on each Cr atom is found to be $3.286 \mu_B$ with opposite spin orientation. This moment mainly comes from the Cr 3*d* orbital as can be seen from the partial DOS of Cr atom in Fig. 2(d), similar to the Cr-doped ZnO bulk case.

Based on our calculations, we found some fundamental differences between the surface and bulk of Cr-doped ZnO. In bulk, Cr substituting Zn atom is fourfold coordinated. The Cr–O bond contracts as compared with the Zn–O bond. However, on the surface, Cr becomes threefold coordinated and Cr–O bond expands by 3.7% when compared with the Zn–O bond length on the surface. To reduce the energy cost for this bond expansion on the surface, Cr atoms prefer to reside far apart from each other. Consequently, Cr atoms do not cluster around O atoms. It has been shown that the FM coupling between Cr atoms in Cr_2O molecule is driven by

TABLE I. Energetics of Cr-doped ZnO slab. The first column identifies the configurations corresponding to different Zn sites that are replaced by Cr (see Fig. 3). The second column shows the optimized Cr–Cr distance $d_{\text{Cr-Cr}}$. The third column gives the energy difference $\Delta\varepsilon$ relative to the ground state (configuration III). The energy difference ΔE between AFM and FM states for each configuration is given in the fourth column. The preferred magnetic coupling between Cr atoms is given in the fifth column.

Configurations	$d_{\text{Cr-Cr}}$ (Å)	$\Delta\varepsilon$ (eV)	ΔE (eV)	Coupling
I(2,4/29,31)	3.336	0.314	0.226	FM
II(2,3/29,32)	5.209	0.713	-0.038	AFM
III(1,2/30,29)	6.142	0.000	-0.025	AFM
IV(2,5/29,28)	3.208	0.857	0.345	FM
V(2,6/29,27)	5.491	0.906	-0.080	AFM
VI(7,6/25,27)	3.244	1.397	0.540	FM
VII(5,6/28,27)	6.106	1.551	-0.033	AFM

the direct Cr 3*d* and O 2*p* exchange interactions.¹⁶ Ferromagnetism shown in Cr-doped ZnO bulk follows a similar picture. This is also found to be true in surface and subsurface configurations where two Cr atoms cluster around O (configuration I, configuration IV, and configuration VI) and like to couple ferromagnetically. However, for these configurations, the energies are higher than the AFM ground state. In the ground state configuration on the surface, O atom does not directly bridge the Cr atoms. Hence the direct *p-d* exchange interaction does not occur and the ferromagnetic coupling is not favored.

In conclusion, we studied the magnetism in (Zn, Cr)O system in both bulk and (10 $\bar{1}$ 0) surface with wurtzite structure. In the bulk case, Cr–Cr coupling is FM and the Cr atoms prefer to cluster around the neighboring O atoms. In the surface case, on the other hand, the coupling is AFM, as Cr atoms no longer prefer to cluster around O. Therefore, the different magnetic coupling between Cr atoms doped in thin film as compared to the bulk case arises from the different morphology associated with Cr doping.

¹K. Ando, T. Hayashi, M. Tanaka, and A. Twardowski, J. Appl. Phys. **83**, 6548 (1998).

²H. Munekata, H. Ohno, S. von Molnar, A. Segmüller, L. L. Chang, and L. Esaki, Phys. Rev. Lett. **63**, 1849 (1989).

³H. Saito, V. Zayets, S. Yanagata, and K. Ando, Phys. Rev. Lett. **90**, 207202 (2003).

⁴K. Sato and H. K. Yoshida, Jpn. J. Appl. Phys., Part 2 **39**, L555 (2000).

⁵E. Kulatov, Y. Uspenskii, H. Mariette, J. Cibert, D. Ferrand, H. Nakayama, and H. Ohta, J. Supercond. **16**, 123 (2003).

⁶Y. Uspenskii, E. Kulatov, H. Mariette, H. Nakayama, and H. Ohta, J. Magn. Magn. Mater. **258-259**, 248 (2003).

⁷K. Ueda, H. Tabata, and T. Kawai, Appl. Phys. Lett. **79**, 988 (2001).

⁸Z. Jin, T. Fukumura, M. Kawasaki, K. Ando, H. Saito, T. Sekiguchi, Y. Z. Yoo, M. Murakami, Y. Matsumoto, T. Hasegawa, and H. Koinuma, Appl. Phys. Lett. **78**, 3824 (2001).

⁹H.-J. Lee, S.-Y. Jeong, J.-Y. Hwang, and C. R. Cho, Europhys. Lett. **64**, 797 (2003).

¹⁰M. delal. Olvera, A. Maldonado, Y. Matsumoto, R. Asomoza, M. Melendez-Lira, and D. R. Acosta, J. Vac. Sci. Technol. A **19**, 2097 (2001).

¹¹I. Satoh and T. Kobayashi, Appl. Surf. Sci. **216**, 603 (2003).

¹²Y. Wang and J. P. Perdew, Phys. Rev. B **44**, 13298 (1991).

¹³G. Kresse and J. Joubert, Phys. Rev. B **59**, 1758 (1999).

¹⁴G. Kresse and J. Furthmüller, Phys. Rev. B **54**, 11169 (1996).

¹⁵H. J. Monkhorst and J. D. Pack, Phys. Rev. B **13**, 5188 (1976).

¹⁶K. Tono, A. Terasaki, T. Ohta, and T. Kondow, Phys. Rev. Lett. **90**, 133402 (2003).

¹⁷Q. Wang, Q. Sun, B. K. Rao, and P. Jena, Phys. Rev. B **69**, 233310 (2004).

¹⁸Q. Wang, Q. Sun, P. Jena, and Y. Kawazoe, Phys. Rev. Lett. **93**, 155501 (2004).